Immunology and Inflammation

Commensal Bacteria Maintain a Qa-1^b-restricted Unconventional CD8$^+$ T Population in Gut Epithelium

Jian Guan ✉, **J. David Peske, Michael Manoharan Valerio, Chansu Park, Ellen A. Robey, Scheherazade Sadegh-Nasseri** ✉, **Nilabh Shastri**

Department of Pathology and the Institute of Cell Engineering, Johns Hopkins University School of Medicine, Baltimore, MD 21287, USA • Division of Immunology and Molecular Medicine, Department of Molecular and Cell Biology, University of California, Berkeley, Berkeley, CA 94720, USA

Reviewed Preprint

Published from the original preprint after peer review and assessment by eLife.

About eLife's process

Reviewed preprint posted
August 29, 2023 (this version)

Sent for peer review
July 6, 2023

Posted to bioRxiv
June 23, 2023

Abstract

Intestinal intraepithelial lymphocytes (IELs) are characterized by an unusual phenotype and developmental pathway, yet their specific ligands and functions remain largely unknown. Here by analysis of QFL T cells, a population of CD8$^+$ T cells critical for monitoring the MHC I antigen processing pathway, we established that unconventional Qa-1^b-restricted CD8$^+$ T cells are abundant in intestinal epithelium. We found that QFL T cells showed a Qa-1^b-dependent unconventional phenotype in the spleen and small intestine of naïve wild-type mice. The splenic QFL T cells showed innate-like functionality exemplified by rapid response to cytokines or antigen, while the gut population was refractory to stimuli. Microbiota was required for the maintenance, but not the initial gut homing of QFL T cells. Interestingly, monocolonization with *Pediococcus pentosaceus,* which expresses a peptide that cross-activated QFL T cells, was sufficient to maintain QFL T cells in the intestine. Thus, microbiota is critical for shaping the Qa-1^b-restricted IEL landscape.

eLife assessment

This is an **important** study that investigates the role of commensal microbes and molecules in the antigen presentation pathway in the development and phenotype of an unusual population of T lymphocytes. The authors provide **convincing** evidence to identify a population of unconventional T cells that exist in the small intestine epithelium, which appear to depend on commensal microbes, and show that a single commensal microbe (that encodes an antigen capable of weakly stimulating these cells) is sufficient to maintain the T cell population.

Introduction

The display of peptides by MHC class I (MHC I) molecules on the cell surface is critical for CD8$^+$ T cell immune surveillance(***Shastri et al., 2002***). Generation of a peptide repertoire which accurately reflects intracellular events, such as viral infection or mutations, relies on a functional

antigen processing and presentation pathway. After cytosolic cleavage of protein precursors and transport of peptides into the endoplasmic reticulum (ER), the peptide intermediates are further customized by ER aminopeptidase associated with antigen processing (ERAAP) until 'ideal' peptides that fit the groove of MHC I molecules are eventually shuttled and displayed on the cell surface(**Blum et al., 2013**; **Serwold et al., 2002**; **Shastri et al., 2005**). Disruption of each step of the pathway can lead to immunological dysfunction(**Grandea et al., 2000**; **Van Kaer et al., 1994**; **Van Kaer et al., 1992**). The critical role of ERAAP in the antigen processing pathway has been established through extensive studies of ERAAP deficient (ERAAP-KO) cells and mice(**Blanchard et al., 2008**; **Guan et al., 2021**; **Hammer et al., 2007b**). Loss of ERAAP severely disrupts the peptide repertoire presented by both the classical MHC Ia and the nonclassical MHC Ib molecules (**Hammer et al., 2006**; **Hammer et al., 2007a**). Qa-1^b, a nonclassical MHC Ib molecule, has been shown to present a significantly increased number of peptides on the cell surface of ERAAP-KO cells as compared with wild-type (WT) cells(**Nagarajan et al., 2016**). One peptide presented by Qa-1^b, FYAEATPML (FL9) (with the Qa-1^b-FL9 complex termed QFL), was identified as an immunodominant ligand uniquely presented on ERAAP-deficient cells(**Nagarajan et al., 2012**). The CD8$^+$ T cells that specifically recognize this ligand are thus named QFL-specific T (QFL T) cells.

Early analysis of QFL T cells revealed the unusual nature of these CD8$^+$ T cells. Unlike conventional antigen-specific CD8$^+$ T cells which are typically detected at a frequency of 1 in 10^5~10^6, QFL T cells are present at a frequency 10-fold higher in the spleen of naïve mice. Interestingly, the bulk splenic QFL T population displayed a CD44^{hi}CD122$^+$ antigen-experienced phenotype(**Nagarajan et al., 2012**). T cell receptor (TCR) analysis of QFL T cells revealed that a large proportion of the QFL T population expresses an invariant TCRα chain Vα3.2Jα21(**Guan et al., 2017**). These traits of QFL T cells indicate their potential similarity to other unconventional T cells, such as invariant NKT (iNKT) and mucosal associated invariant T(MAIT) cells, which are typically characterized by recognition of ligands present by non-classical MHC Ib, expression of invariant TCRs, residence in nonlymphoid tissues and innate-like functions(**Godfrey et al., 2015**; **Salio et al., 2014**). The tissue distribution and functions of QFL T cells remains to be fully elucidated.

The gut mucosa is an immunologically complex niche with abundant lymphoid populations(**Faria et al., 2017**). The small intestinal intraepithelial lymphocyte (siIEL) compartment is populated by unconventional T cells of both TCRγδ$^+$ and TCRαβ$^+$ lineage with characteristic CD8αα expression. The development of the CD8αα$^+$CD4$^-$CD8αβ$^-$TCRαβ$^+$ population (CD8αα$^+$ IEL), categorized as natural IELs (natIELs) because they acquire their activated phenotype in the thymus, has been extensively studied (**Cheroutre et al., 2011**). Yet little is known about their antigen specificity and TCR repertoire. Emerging evidence shows that nonclassical MHC Ib molecules are important for the development and effector function of CD8αα$^+$ IELs(**Das et al., 2003**). For instance, while loss of classical MHC Ia molecules showed little impact on the CD8αα$^+$ IEL population, these cells were decreased in mice deficient for Qa-2 (**Das et al., 2000**; **Das et al., 1999**; **Park et al., 1999**). Furthermore, a population of CD8αα$^+$ IEL precursors which preferentially expresses Vα3.2 was shown to be decreased in number in the absence of CD1d(**Ruscher et al., 2017**). However, whether Qa-1^b is involved in shaping the CD8αα$^+$ IEL population remains to be studied. In addition to MHC molecules, gut microbiota plays a critical role in the establishment and shaping of the gut immune system. Studies of germ-free (GF) mice have shown extensive defects in gut-associated lymphoid tissues together with morphological changes in the intestine associated with the absence of gut microbiota(**Round et al., 2009**). Notably, despite the critical role of gut microbiota in the establishment of the gut immune system, natIELs that do not rely on cognate antigens in the periphery are believed to home to the gut independent of microbes(**Mota-Santos et al., 1990**).

Here we found abundant unconventional QFL T cells in both the spleen and siIEL compartment of naïve WT mice. The splenic Vα3.2$^+$QFL T cells expressed high level of CD44 and showed typical innate-like functions including hyperresponsiveness to cytokines and rapid IFN-ɣ production in response to antigen. In contrast, the population of the same antigen specificity in the gut phenotypically resembled natIEL and were likewise functionally quiescent. Analysis of mice deficient of molecules associated with Qa-1^b-FL9 antigen presentation revealed that TAP was required from the presence of the splenic or siIEL QFL T cells, whereas Qa-1^b was essential for imprinting their unconventional phenotype. Furthermore, analysis of GF mice showed that gut microbiota was needed for the long-term maintenance of QFL T cells. Interestingly, we found that maintenance of the gut Vα3.2$^+$QFL T was associated with colonization by the commensal bacterium *Pediococcus pentosaceus* (*P. pentosaceus*) which expresses an FL9 homologue that could cross-activate QFL T cells. Overall, these results establish Vα3.2$^+$QFL T cells as a unique population of unconventional CD8$^+$ T cells that rely on nonclassical MHC Ib to acquire their phenotype, and gut microbiota to be properly maintained in the intestine.

Results

Vα3.2$^+$QFL T cells are abundant in the spleen and gut of naïve wild-type mice

To identify QFL T cells in tissues of naïve WT mice, we generated Qa-1^b-FL9 dextramers (QFL-Dex) based on the 'dextran-doping' technique(***Bethune et al., 2017***). In comparison with Qa-1^b-FL9 tetramers (QFL-Tet), QFL-Dex showed improved sensitivity and specificity for QFL T cell detection (**Supplementary Fig. 1**), and further allowed enrichment of QFL T cells using magnetic beads. The average number of QFL T cells – defined as CD45$^+$CD19$^-$TCRβ$^+$CD4$^-$QFL-Dex-PE$^+$APC$^+$ (**Fig.1 a**) – detected in the siIEL compartment of naïve WT mice was comparable to the population in the spleen. Strikingly, however, QFL T cells were present at a frequency of ~1 in 1,000 of the siIEL CD8$^+$ T cells, which was 10 times more frequent than in the spleen (**Fig.1 b, c**). Both the splenic and siIEL QFL T cells were essentially all CD8$^+$ T cells, as these cells were barely detectable within the CD4$^+$ T population (**Supplementary Fig. 2**). Consistent with prior studies, ~80% of the splenic QFL T cells expressed the 'invariant' TCR Vα segment Vα3.2 which was significantly higher than the proportion of Vα3.2-expressing cells within the total CD8$^+$ T population in the spleen (<5%) (**Fig.1 d, e**) (***Guan et al., 2017***). Interestingly, the QFL T cells in the siIEL compartment also contained a relatively larger proportion of Vα3.2$^+$ cells (~60%) compared to the total CD8$^+$ TCRαβ siIELs (<30%) (**Fig.1 f, g**). The average percentage of Vα3.2$^+$ cells within the QFL T population (20.1%) was lower in the siIEL compartment than in the spleen (63.3%). Vα3.2$^+$ QFL T cells were nevertheless abundantly present in both the spleen and gut of naïve WT mice.

The unconventional phenotype of Vα3.2$^+$QFL T cells

We have previously observed a high percentage of CD44^{hi} cells within the bulk splenic QFL T population of naïve WT mice(***Guan et al., 2017***; ***Nagarajan et al., 2012***). Here we further investigated the association between preferred Vα3.2 usage by QFL T cells and their phenotype. Strikingly, we observed that Vα3.2$^+$QFL T cells contained a significantly larger proportion of CD44^{hi} cells (~90%) than the Vα3.2$^-$QFL T cells, suggesting that the antigen experienced phenotype of the QFL T population was mainly contributed by the Vα3.2-expressing subpopulation (**Fig.2 a, b**). In contrast, only around 20% of the total Vα3.2$^+$CD8$^+$ T population expressed high CD44. Interestingly, the percentage of CD44^{hi} cells within the total Vα3.2$^+$CD8$^+$ T population was slightly higher compared to the Vα3.2$^-$ population (**Supplementary Fig. 3 a**), which was in line with a previous report (***Prasad et al., 2021***). We thus conclude that although both Vα3.2$^+$ and Vα3.2$^-$ cells were detected within the splenic QFL T population, a memory phenotype was specifically enriched in Vα3.2$^+$QFL T cells.

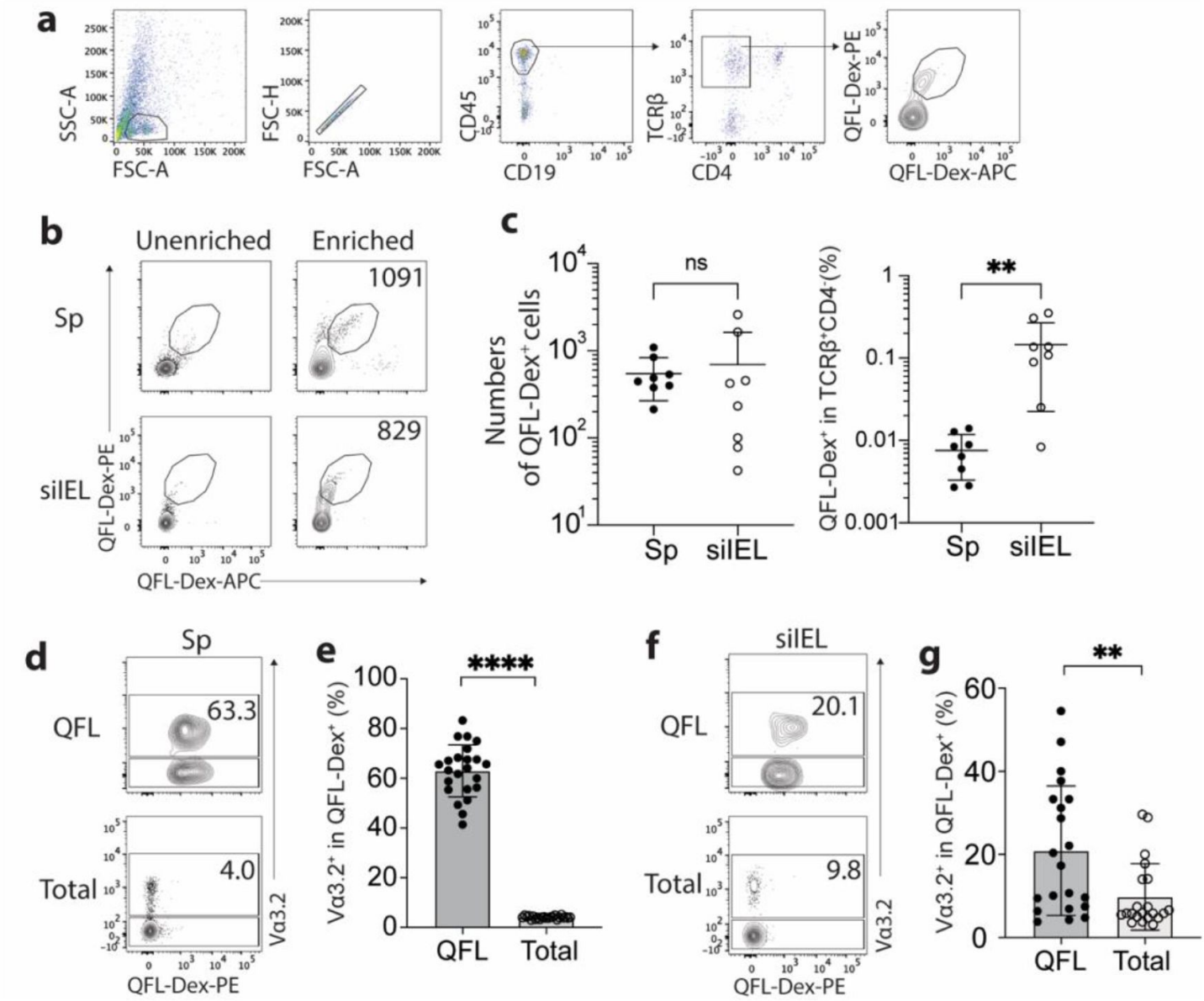

Figure 1

Abundant Vα3.2$^+$ QFL T cells in both the spleen and siIEL compartment of naïve WT mice.

(**a**) Definition of QFL T cells by flow cytometry. Cells from the spleen or siIEL compartment were stained with Qa-1^b-FL9 (QFL) dextramers labeled with phycoerythrin (QFL-Dex-PE) or allophycocyanin (QFL-Dex-APC) and analyzed for before (Unenriched) or after (Enriched) magnetic enrichment of dextramer-positive cells. QFL T cells are defined as the CD45$^+$CD19$^-$TCRβ$^+$CD4$^-$QFL-Dex-PE$^+$APC$^+$ population. Plots representing siIELs from naïve WT mice after enrichment for QFL-Dex$^+$ cells. (**b**) Flow cytometry of cells from the spleen (Sp) and siIEL compartment of naïve WT mice 'Unenriched' or 'Enriched' for dextramer-positive cells. Numbers in plots indicate absolute numbers of QFL-Dex$^+$ cells detected after enrichment. (**c**) Absolute numbers (left) and frequencies (right) of QFL-Dex$^+$ cells detected (as in **b**) among TCRβ$^+$CD4$^-$ population in the spleen or siIEL compartment. **P=0.0069 (**d, f**) Analysis of Vα3.2 expression on QFL-Dex$^+$(QFL) or total CD8$^+$ T (Total) cells from the spleen (**d**) or the siIEL compartment (**f**). Numbers in plots indicate average percentages of Vα3.2$^+$ cells within the indicated populations. (**e**) Frequencies of Vα3.2$^+$ cells detected as in **d.** ****P<0.0001 (**g**) Frequencies of Vα3.2$^+$ cells detected as in **f.** **P=0.0058 Representative data are shown in flow plots (**a, b, d, f**) and the number of replicates is specified in the bar graphs (**c, e, g**). Each symbol represents data collected from the indicated tissue isolated from an individual mouse. P values were calculated with Student's *t* test. 'ns' indicates the comparison was not significant.

Given the strikingly high frequency of QFL T cells in the gut, we further investigated their phenotype. We assessed CD8αα expression, a hallmark of the unconventional phenotype of natIELs, on Vα3.2$^+$ and Vα3.2$^-$ QFL T cells in the siIEL compartment of naïve WT mice. A relatively larger fraction of Vα3.2$^+$QFL T cells lacked CD4 and CD8αβ expression but expressed CD8αα compared to the Vα3.2$^-$ subpopulation suggesting that the majority of Vα3.2$^+$ QFL T cells were CD8αα$^+$ natIELs (**Fig.2 c, d**). No such difference was observed between the total Vα3.2$^+$ and Vα3.2$^-$ CD8$^+$ IEL populations (**Supplementary Fig. 3 b**). These observations indicate that the Vα3.2$^+$ QFL T cells in both the spleen and siIEL compartment are unconventional CD8$^+$ T cells which likely are derived from the same precursors in thymus.

The impact of Qa-1^b, ERAAP, and TAP on Vα3.2$^+$QFL T cells

We further investigated what drives the unconventional phenotype of Vα3.2$^+$ QFL T cells by analyzing mice deficient of molecules that impact Qa-1^b-FL9 antigen presentation including Qa-1^b, ERAAP or TAP (Qa-1^b-KO, ERAAP-KO, TAP-KO). While we consistently observed loss of both the splenic and siIEL Vα3.2$^+$QFL T cells in TAP-KO mice, the populations were detectable in both tissues of Qa-1^b-KO or ERAAP-KO mice with a slightly reduced population size in the spleen of Qa-1^b-KO mice (**Fig.3 a**). Strikingly, Vα3.2$^+$ QFL T populations showed reduced percentages of CD44^{hi} cells in the spleen of Qa-1^b and ERAAP deficient mice with the reduction being more significant in Qa-1^b-KO mice. In contrast, the phenotype of splenic Vα3.2$^-$ QFL T cells was not significantly affected (**Fig.3 b, c**). Interestingly, similar pattern of phenotype change was observed for the siIEL Vα3.2$^+$ QFL T cells which showed almost complete loss of the unconventional natIEL phenotype including CD8αα expression in Qa-1^b-KO mice (**Fig.3 d, e**, **Supplementary Fig. 4**). These results demonstrate that TAP and Qa-1^b both play a role in the establishment of the unconventional Vα3.2$^+$ QFL T population, with TAP being required for the presence of the population, and Qa-1^b being required for the unconventional phenotype imprinting of these cells. Paradoxically, loss of ERAAP, which would be expected to increase the presentation of FL9, also led to a reduction of memory and unconventional phenotypes in QFL T cells, perhaps due to the loss of high affinity QFL T clones due to tolerance mechanisms, such as negative selection. It is also worth noting that total splenic Vα3.2$^+$CD8αβ$^+$ T cells showed a similar loss of memory phenotype in Qa-1^b-KO and ERAAP-KO mice, whereas Vα3.2$^-$ CD8αβ$^+$T cells did not (**Supplementary Fig. 3 c**). Thus, the unconventional Vα3.2$^+$QFL T cells specifically, and a substantial proportion of total Vα3.2$^+$ splenocytes, are impacted by Qa-1^b and ERAAP.

Vα3.2$^+$QFL T cells are functionally innate-like in the spleen but quiescent in gut

To further investigate the functional features of Vα3.2$^+$QFL T cells, we utilized transgenic mice (QFLTg) expressing the predominant invariant TCR found on QFL T cells (*Vα3.2Jα21, Vβ1Dβ1Jβ2-7*), referred to hereafter as QFLTg cells. Abundant QFLTg cells or control OT-1 cells were detected in both the spleen and siIEL compartment of the respective TCR transgenic mice (**Supplementary Fig. 5 a**). Phenotypically, the QFLTg cells recapitulated the unconventional phenotype of polyclonal Vα3.2$^+$QFL T cells with high CD44 expression in the spleen and CD8αα expression in the siIEL compartment. In contrast, OT-1 cells were phenotypically similar to conventional naïve CD8$^+$ T cells, as they expressed low to intermediate levels of CD44 in the spleen and lacked CD8αα expression in gut (**Supplementary Fig. 5 b, c**).

Cytokines including IL15 and the combination of IL7/IL18 have been implicated in the maintenance and survival of both 'virtual' memory T cells and IELs (***Klose et al., 2014***; ***Okazawa et al., 2004***; ***Prasad et al., 2021***; ***Schluns et al., 2003***). We thus compared the proliferation of QFLTg and OT-1 cells in response to these cytokines. In keeping with their virtual memory surface marker phenotype, splenic QFLTg cells were significantly more responsive to IL15 or IL7/IL18 stimulation than OT-1 cells (**Fig.4 a**). At 72hs, ~80% of QFLTg cells had proliferated in

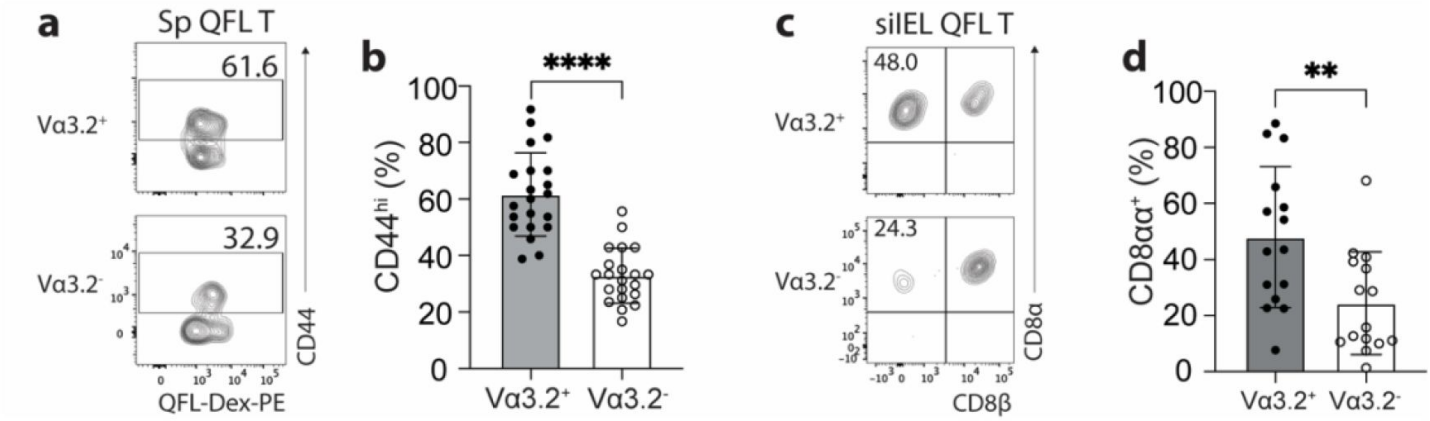

Figure 2

The unconventional phenotype of Vα3.2$^+$ QFL T cells.

(**a**) Analysis of CD44 expression on Vα3.2$^+$ or Vα3.2$^-$ QFL-Dex$^+$ cells enriched from the spleen of naïve WT mice. Numbers in plots indicate average percentages of CD44^{hi} cells detected among the Vα3.2$^+$ or Vα3.2$^-$ QFL-Dex$^+$ populations. (**b**) Frequencies of CD44^{hi} cells detected as in **a**.****P<0.0001 (**c**) Analysis of CD8α and CD8β expression on Vα3.2$^+$ or Vα3.2$^-$ QFL-Dex$^+$ cells enriched from the siIEL compartment of naïve WT mice. Numbers in plots indicate average percentages of CD8αα$^+$ cells detected among the Vα3.2$^+$ or Vα3.2$^-$ QFL-Dex$^+$ populations. (**d**) Frequencies of CD8αα$^+$ cells detected as in **c.** **P=0.0065 Samples of <20 cells in the Vα3.2$^+$QFL-Dex$^+$ gate were excluded in the phenotype analysis. Representative data are shown in flow plots (**a, c**) and the number of replicates is specified in the bar graphs (**b, d**). Each symbol represents data collected from the indicated tissue isolated from an individual mouse. P values were calculated with Student's *t* test. 'ns' indicates the comparison was not significant.

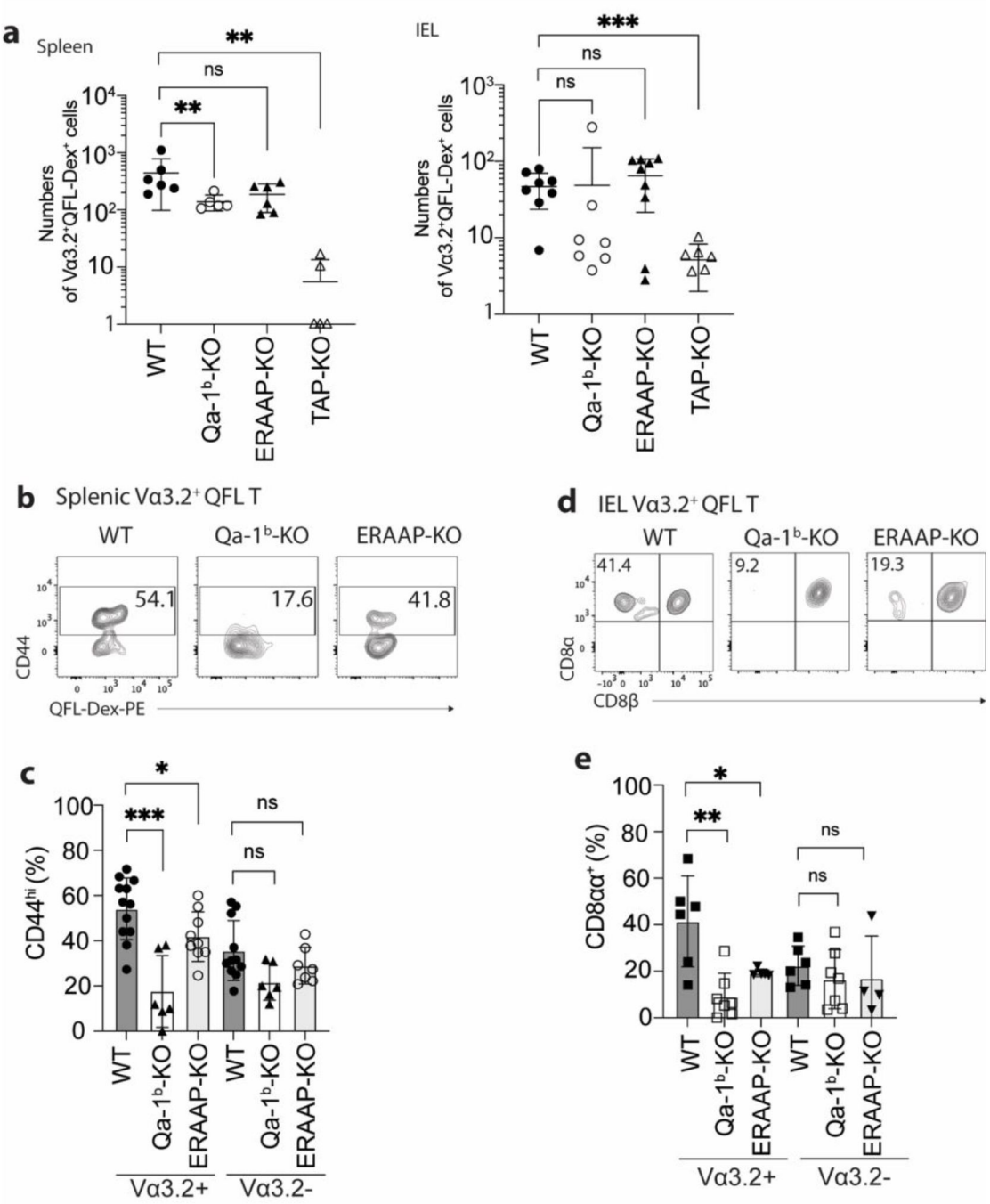

Figure 3

Phenotype of Vα3.2$^+$ QFL T cells in mice of various genotypes.

(**a**) Absolute numbers of Vα3.2$^+$QFL-Dex$^+$ cells detected in the spleen (left) or siIEL compartment (right) of Qa-1^b, ERAAP or TAP deficient (Qa-1^b-KO, ERAAP-KO or TAP-KO) mice in comparison with WT mice.** P<0.009 ***P=0.0006 Symbols on x-axis indicate that the cells were undetectable in TAP-KO mice. (**b**) Analysis of CD44 expression on splenic Vα3.2$^+$QFL-Dex$^+$ cells enriched from naïve WT, Qa-1^b-KO or ERAAP-KO mice. Numbers in plots indicate average percentages of CD44^{hi} cells. (**c**) Frequencies of CD44^{hi} cells detected among Vα3.2$^+$(as in **b**) or Vα3.2$^-$ QFL T cells.***P=0.0004 *P=0.0388 (**d**) Flow cytometry analysis of CD8α and CD8β expression on the Vα3.2$^+$QFL-Dex$^+$ cells enriched from the siIEL compartment of naïve WT, Qa-1^b-KO or ERAAP-KO mice. Numbers in plots indicate average percentages of CD8αα$^+$ cells. (**e**) Percentages of CD8αα$^+$ cells detected among Vα3.2$^+$(as in **d**) or Vα3.2$^-$ QFL T cells. **P=0.0082 *P=0.0335 Representative data are shown in flow plots (**b, d**) and the number of replicates is specified in the bar graphs (**a, c, e**). Each symbol represents data collected from the indicated tissue isolated from an individual mouse. P values were calculated with Student's *t* test. 'ns' indicates the comparison was not significant.

response to the cytokines, compared with only ~50% of OT-1 cells (**Fig.4 b**). Interestingly, T cells isolated from the siIEL compartment of QFLTg or OT-1 mice showed a distinct pattern of cytokine responsiveness from the splenic T cells. First, both QFLTg and OT-1 cells from siIEL were less responsive to IL15 than the splenic population. Second, siIEL QFLTg cells showed significantly reduced proliferation in response to the cytokines, especially to the combination of IL7/IL18, as compared with OT-1 cells (**Fig.4 c, d**).

To ensure that altered effector function was not skewed by the high specific TCR frequency in TCR transgenics, we generated partial hematopoietic chimeric mice with physiological precursor frequencies (QFLTg_WT) by transferring bone marrow cells from GFP^+QFLTg mice into nonirradiated naïve WT neonates(***Ladi et al., 2008***). OT-1_WT chimera mice were generated in parallel as representative of conventional $CD8^+$ T cells (**Fig.4 e**). This experimental design allowed us to track the GFP^+ donor-derived T cells ($GFP^+CD45^+CD19^-TCR\beta^+CD4^-V\alpha3.2^+$) separately from the recipient's endogenous T cells (**Fig.4 f**). Based on the hyperresponsiveness of splenic QFLTg cells to cytokines, we hypothesized that these cells would exert effector functions more rapidly than conventional CD8 T cells, similar to the known innate-like T cells such as iNKT. We measured IFN-ɣ production by QFLTg or OT-1 cells from splenocytes or siIEL cells of naïve QFLTg_WT or OT-1_WT chimera mice stimulated the with 2μM FL9 or SIINFEKL(SL8) peptide respectively for 4.5 hours directly *ex vivo*. A strikingly large fraction (~60%) of splenic QFLTg cells expressed high levels of IFN-ɣ under these conditions, while only 6% of OT-1 cells did so (**Fig.4 g, h**). Notably, despite the low responsiveness to epitopes, siIEL QFLTg cells showed relatively higher basal levels of IFN-ɣ expression than OT-1 cells (**Fig.4 i, j**). In contrast to the hyperresponsiveness of splenic QFLTg cells to their ligand, neither QFLTg nor OT-1 cells from the siIEL compartment showed significant IFN-ɣ production at 4.5 hours. The low IFN-ɣ production of IEL QFLTg cells was in keeping with their natIEL phenotype - antigen-experienced yet functionally quiescent(***Cheroutre et al., 2011***; ***Denning et al., 2007***). We conclude that $V\alpha3.2^+$QFL T cells in the spleen are functionally innate-like, whereas the population with the same TCR specificity in the small intestine shows functional features of natIEL.

Gut microbiota is associated with retention but not homing of QFL T cells

The establishment and function of the intestinal immune system is intimately associated with homeostasis of the gut microbial community, as evidenced by an altered gut immune cell composition in germ-free (GF) mice (***Belkaid et al., 2014***; ***Macpherson et al., 2004***; ***Round and Mazmanian, 2009***). To investigate if an association exists between gut microbiota and gut QFL T cells, we compared the numbers and frequencies of QFL T cells in the spleen and siIEL compartment of naïve specific-pathogen-free (SPF) and GF WT mice of various ages. First, we found the absolute number of QFL T cells in the spleen was unaffected by the absence of gut microbiota in either young or old mice. The frequency of QFL T cells was relatively higher in GF than in SPF mice, as a result of a decreased number of non-QFL $CD8^+$ T cells in the spleen of GF mice (**Fig.5 a, b**). Interestingly, the percentage of $CD44^{hi}$ cells within the total $CD8^+$ T population was proportionally higher in the spleen of GF WT than in SPF WT mice regardless of their Vα3.2 expression (**Supplementary Fig. 6 a**). This observation suggested that gut microbiota might be more closely associated with the presence of conventional naïve $CD8^+$ T cells rather than the memory phenotype $CD8^+$ T population in the spleen. Second, while the number and frequency of QFL T cells in siIEL compartment showed no significant difference between GF and SPF mice of relatively young age (8~17-week), the population was gradually lost in old GF mice (18~22-week) (**Fig.5 c, d**), with the decrease in GF mice starting from around 16 weeks of age (data not shown). In addition, the QFL T cells detected in the spleen or siIEL compartment of young SPF or GF mice showed similar expressions of Vα3.2, CD44 and CD8αα (**Supplementary Fig. 7**). We conclude that although QFL T cells could home to gut in the absence of microbiota, microbe-derived antigens or signals are required for their maintenance there. Interestingly, we observed that the average percentage of $CD8\alpha\alpha^+$ cells among the total $TCR\beta^+CD4^-$ T population was

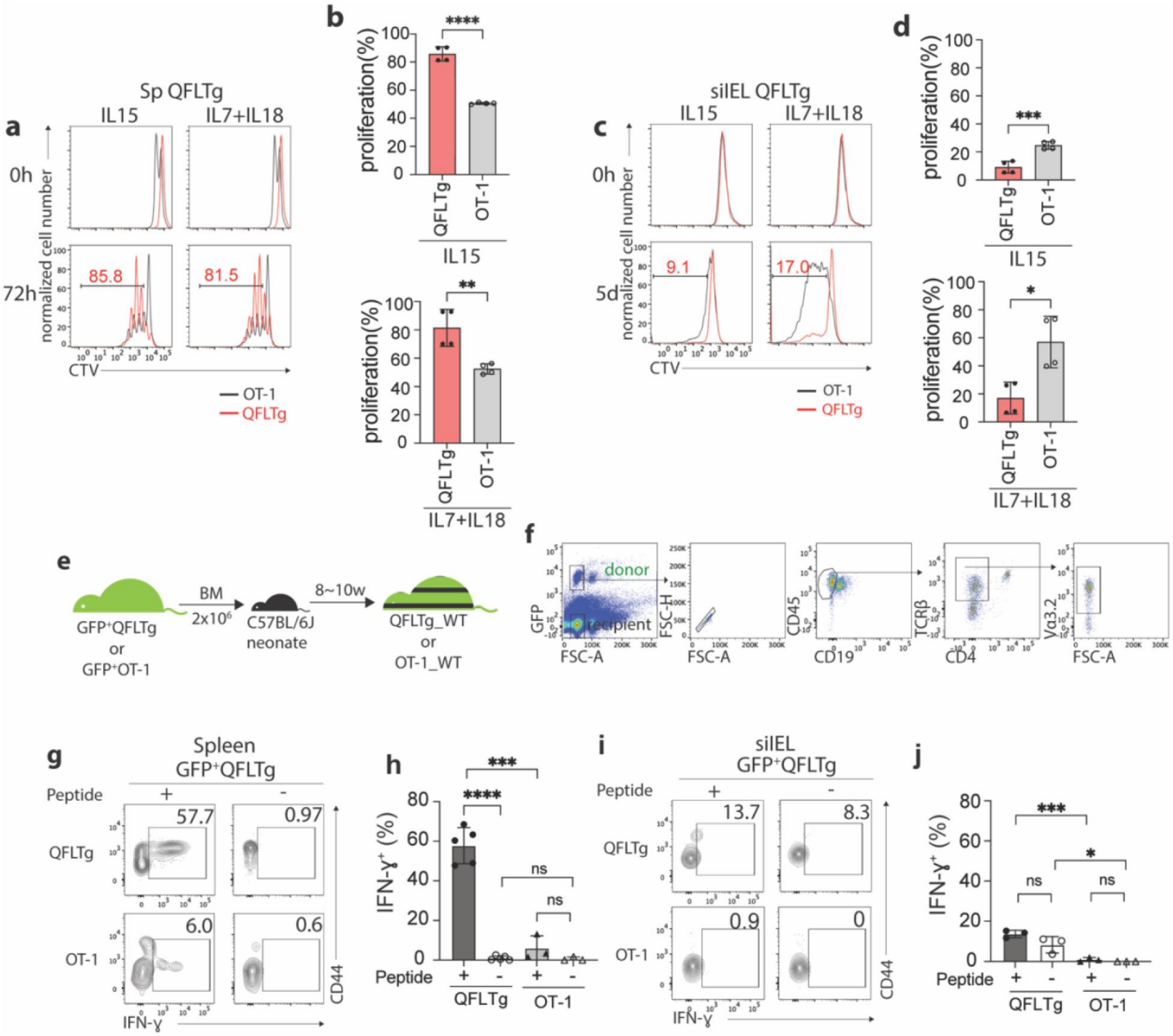

Figure 4

Distinct functional features of QFLTg cells in the spleen and gut.

(**a, c**) Proliferation of splenic (**a**) or siIEL (**c**) QFLTg or OT-1 cells from QFLTg or OT-1 mice in response to IL15 (left) or a combination of IL7 and IL18 (right) stimulation. Cells were tracked using Cell Tracing Violate (CTV). Numbers in plots indicate average percentages of proliferated QFLTg cells. (**b**) Percentages of proliferated splenic QFLTg or OT-1 cells as detected in **a**. ****P<0.0001 **P=0.0052 (**d**) Percentages of proliferated siIEL QFLTg or OT-1 as detected in **c**. ***P=0.0009 *P=0.0101 (**e**) Generation of QFLTg_WT or OT-1_WT partial hematopoietic chimera mice. 2×10^6 of the bone marrow (BM) cells from GFP^+QFLTg or GFP^+OT-1 mice were transferred into WT neonates at 3~5 days of age. The chimera mice were analyzed at 8~10 weeks of age. (**f**) Gating strategy for the QFLTg cells originated from donor bone marrow cells in QFLTg_WT chimera mice. Plots representing donor-derived QFLTg population in the spleen being gated as $GFP^+CD45^+CD19^-TCR\beta^+CD4^-V\alpha3.2^+$ cells. (**g, i**) Flow cytometry measurement of IFN-γ production by QFLTg or OT-1 cells isolated from the spleen (**g**) or siIEL compartment (**i**) of naïve chimera mice stimulated with or without 2μM FL9 or SL8 peptide respectively for 4.5h. Numbers in plots indicate average percentages of IFN-γ^+ cells. (**h**) Percentages of IFN-γ^+ cells detected as in **g**. ****P<0.0001 ***P=0.0001 (**j**) Percentages of IFN-γ^+ cells detected as in **i**. ***P=0.0004 *P=0.0247 Representative data are shown in flow plots (**a, c, f, g, i**) and the number of replicates is specified in the bar graphs (**b, d, h, j**). Each symbol represents data collected from the indicated tissue isolated from an individual mouse. P values were calculated with Student's *t* test. 'ns' indicates the comparison was not significant.

proportionally larger in GF mice than SPF mice regardless of Vα3.2 expression, although the Vα3.2$^-$ population showed a more significant increase (**Supplementary Fig. 6 b**). This was mainly a result of a decreased number of CD8αβ$^+$ T cells in the siIEL of GF mice (data not shown). Nevertheless, here we showed that Qa-1^b restricted T cells could home to the small intestine epithelium and display a natIEL phenotype independent of gut microbiota.

QFL T cells cross-react with a microbial antigen and are retained in gut by a commensal bacterium

We next investigated how the QFL T population was retained in the gut of SPF WT mice, hypothesizing that the presence of specific antigen might play a role. QFL T cells specifically recognize the Qa-1^b-FL9 complex which is uniquely presented on ERAAP deficient cells. Because it is unlikely this ligand is constantly presented in gut epithelium under homeostatic conditions (**Supplementary Fig. 8 a**), we reasoned that QFL T cells might be retained in the gut through exposure to FL9 homologue peptide(s) expressed by commensal bacteria that colonize small intestine.

To identify potentially cross-reactive peptides, we first determined the key residues of the FYAEATPML(FL9) peptide that affected TCR recognition by QFL T cells. Due to the lack of structural information on QFL-TCR complex, we hypothesized that the glutamic acid at P4 and threonine at P6 were likely to be critical based on the nature and position of amino acids. The QFL T hybridoma cell line BEko8Z which expresses TCR-induced β-galactosidase (LacZ) was used to test whether FL9 peptide variants with the hypothesized key residues substituted by alanine altered T cell responses. By measuring the LacZ production of BEko8Z cells in response to Qa-1^b-expressing Lmtk$^-$ (L-Qa-1^b) cells pulsed with FYAAATPML(FL9-P4A) or FYAEAAPML(FL9-P6A), we found that replacement of the P6 threonine reduced TCR recognition, while replacement of the P4 glutamic acid led to the complete loss of the BEko8Z response (**Supplementary Fig. 8 b**). We thus conclude that both the P4 and P6 positions are important with the P4 glutamic acid being particularly critical for QFL T recognition.

To identify potential bacterial FL9 homologous peptides, we aligned the FL9 peptide sequence with proteomes of the five dominant gut commensal bacterial phyla, including Actinobacteria, Bacteroidetes, Firmicutes, Proteobacteria, Verrucomicrobia from the NCBI Swissprot Non-redundant UniProtKB database(***Donaldson et al., 2016***). The alignment result was further curated to 30 candidate peptides based on their homology with FL9 peptide at position P4 and P6 (**Supplementary Fig. 8 c, Supplementary Table.1**). By measuring the LacZ production of BEko8Z cells in response to L-Qa-1^b cells pulsed with 50nM of each of the candidate peptides, we identified a single stimulatory peptide FYAEDGTPIL (FL10) that is expressed in *P. pentosaceus*, a gram-positive lactic acid bacteria(LAB) that colonizes the small intestine (**Fig.6 a**). Sensitivity to the FL9 peptide was ~1,000 fold greater than to FL10, but BEko8Z cells could recognize FL10 at concentrations as low as 1.5nM. In contrast, FYAEDDTPIV(FV10), a FL10 homologous peptide expressed in *Lactobacillus johnsonii* which is a common LAB that colonize GI tract, failed to activate BEko8Z cells (**Fig.6 b**, **Supplementary Fig. 8 d**).

To further investigate the association between *P. pentosaceus* and Vα3.2$^+$QFL T cells in gut, we first generated QFLTg_WT partial hematopoietic chimeras using germ-free WT mice (GF QFLTg_WT) and monocolonized the GF chimera mice with *P. pentosaceus* at 8 weeks of age. The mice were analyzed 8 weeks later (**Fig.6 c**). The donor-derived QFLTg cells and the recipient-derived Vα3.2$^+$QFL T cells were distinguished by GFP expression and further defined as the CD45$^+$CD19$^-$ TCRβ$^+$CD4$^-$Vα3.2$^+$QFL-Dex-PE$^+$ population on flow cytometry as was described earlier. While the donor-derived QFLTg populations were present and phenotypically unaltered in the spleen and siIEL compartment of GF QFLTg_WT chimera mice at 8 weeks of age, they were barely detectable in the GF chimera mice at 16 weeks of age (**Supplementary Fig. 9**, **Fig.6 d**). Strikingly,

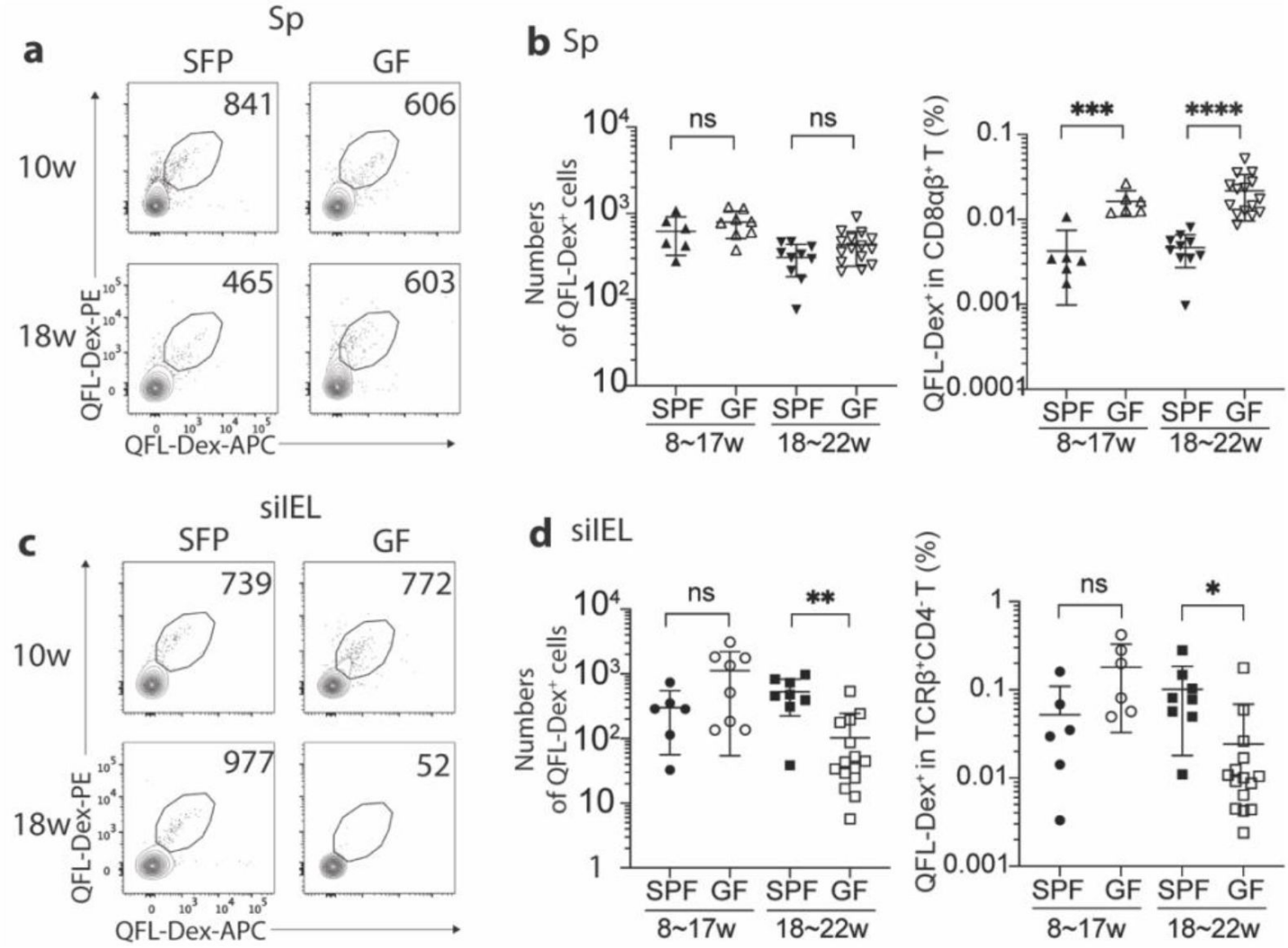

Figure 5

Gut microbiota is associated with retention but not homing of QFL T cells in the siIEL compartment.

(**a, c**) Flow cytometry of QFL-Dex$^+$ cells enriched from the spleen (**a**) or siIEL compartment (**c**) of specific-pathogen-free (SPF) or germ-free (GF) WT mice at 10 or 18 weeks of age. Numbers in plots indicate absolute numbers of QFL-Dex$^+$ cells. (**b**) Absolute numbers (left) and frequencies (right) of QFL-Dex$^+$ cells detected within the total splenic CD8$^+$ population in SPF or GF WT mice of 8~17 weeks or 18~22 weeks of age.***P=0.009 ****P<0.0001 (**d**) Absolute numbers and frequencies of QFL-Dex$^+$ cells detected among the total siIEL TCRβ$^+$CD4$^-$ population in SPF or GF WT mice of 8~17 weeks or 18~22 weeks of age. **P=0.005 *P=0.037 Representative data are shown in flow plots (**a, c**) and the number of replicates is specified in the bar graphs (**b, d**). Each symbol represents data collected from the indicated tissue isolated from an individual mouse. P values were calculated with Student's *t* test. 'ns' indicates the comparison was not significant.

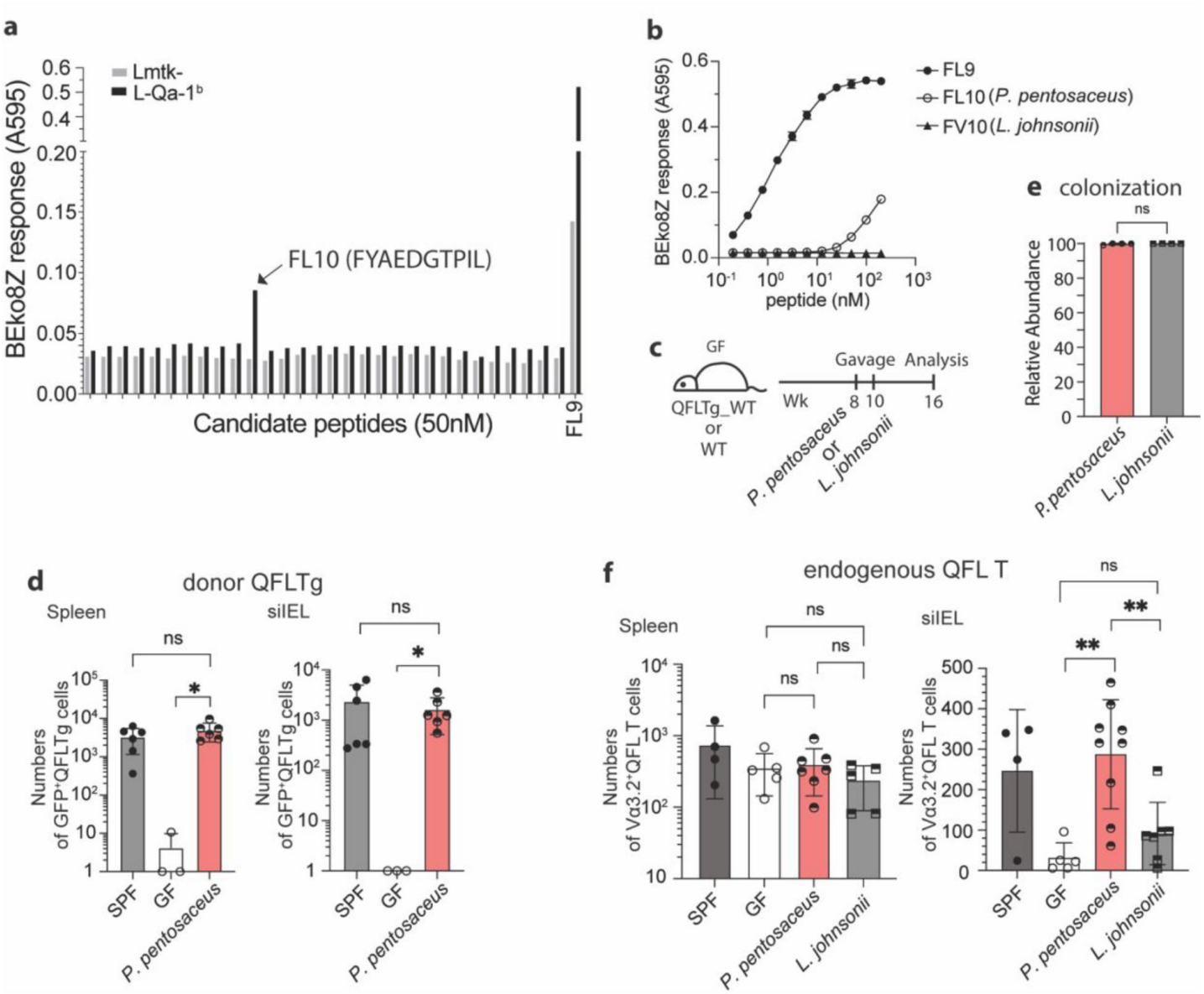

Figure 6

Association between Vα3.2$^+$QFL T cells and the commensal bacterium *P. pentosaceus*.

(**a**) Identification of the QFL T cross-reactive peptide FYAEDGTPIL(FL10). LacZ response of BEko8Z hybridoma cells to the Qa-1^b-expressing Lmtk$^-$ (L-Qa-1^b) cells or the non-Qa-1^b-expressing Lmtk$^-$ cells pulsed with 50nM of the candidate FL9 or its homolog peptides measured by spectrophotometry. (**b**) Response of BEko8Z hybridoma to L-Qa-1^b cells pulsed with FL9, FL10 or FYAEDDTPIV (FV10) peptide of various concentrations. (**c**) Colonization of GF mice with commensal bacteria. GF QFLTg_WT chimera mice received oral gavage of *P. pentosaceus* at 8 weeks of age and were analyzed for both the donor-derived QFLTg cells and the endogenous Vα3.2$^+$QFL T cells at 16 weeks of age. GF WT mice received oral gavage of *P. pentosaceus* or *L. johnsonii* at 8 and 10 weeks of age and were analyzed for the endogenous Vα3.2$^+$QFL T cells at 16 weeks of age. (**d**) Absolute numbers of donor-derived QFLTg cells in the spleen (left) or siIEL compartment (right) of 16-week GF QFLTg_WT chimera mice colonized with *P. pentosaceus* in comparison with SPF or uncolonized GF chimera mice. Symbols on x-axis indicate that QFLTg cells were undetectable in the indicated group. *P<0.03 (**e**) Relative abundance of *P. Pentosaceus* or *L. Johnsonii* determined by whole shotgun metagenomic sequencing of microbiota composition in pooled fecal pallets collected from each cage. (**f**) Absolute numbers of endogenous Vα3.2$^+$QFL T cells in the spleen (left) or siIEL compartment (right) of 16-week colonized GF mice compared with SPF or uncolonized GF chimera mice. Endogenous Vα3.2$^+$QFL T data collected from the GF QFLTg_WT chimeric mice and the non-chimeric WT mice were pooled for this analysis. **P<0.008 (**a, b**) Data are from one experiment representative of three experiments. The number of replicates is specified in the bar graphs with each symbol representing data collected from the indicated sample/tissue isolated from an individual cage (**e**) or mouse (**d**, **f**). P values were calculated with Student's *t* test. 'ns' indicates the comparison was not significant.

monocolonization of the GF QFLTg_WT chimera mice with *P. pentosaceus* completely restored the donor-derived QFLTg population in both tissues in 16-week GF chimera mice (**Fig.6 d**). We then further tested whether restoration of the gut QFL T population was specifically associated with *P. pentosaceus* by monocolonizing GF WT mice with *P. pentosaceus* or *L. johnsonii* (**Fig.6 c**). Analysis of the microbiome composition of fecal pallets showed that both species efficiently colonized the GF mice (**Fig.6 e**). While the endogenous Vα3.2$^+$QFL T population in the siIEL compartment was retained by *P. pentosaceus* colonization of GF mice at 16 weeks of age, *L. johnsonii* colonization failed to restore the population to level comparable with SPF or *P. pentosaceus* colonized mice. On the other hand, maintenance of the endogenous splenic QFL T population was independent of microbes, in line with our earlier observations (**Fig.6 f**). Donor-derived QFLTg and endogenous Vα3.2$^+$QFL T cells in the spleen likely showed discrepant results due to different sources of precursors for the two populations. Unlike the endogenous populations which were constantly replenished, the donor-derived QFLTg cells rose from a fixed number of bone marrow cells, and gradually decreased in number as the animal age (**Supplementary Fig. 10**). Thus, presence of the ligand which was supplied by peptide derived from *P. pentosaceus* might be required for the donor-derived QFLTg cells to be retained in the spleen, whereas the endogenous splenic population was unaffected by microbes. Phenotype analysis revealed that both the donor-derived QFLTg cells and the endogenous Vα3.2$^+$QFL T cells from the colonized GF chimera mice showed a memory phenotype identical to that seen in the SPF chimera mice (**Supplementary Fig. 11**). We thus conclude that the late-life maintenance of Vα3.2$^+$QFL T cells in the small intestine was dependent on the commensal bacterium *P. pentosaceus* which expresses a FL9 homologue peptide. While the presence of the bacterial FL10 peptide likely plays an important role in retention of gut QFL T cells, we do not exclude the possible contributions of other commensal bacterial factors. In addition, the unconventional phenotype of QFL T cells was likely acquired through microbe-independent mechanisms.

Discussion

The small intestine epithelium harbors a highly heterogenous intraepithelial lymphocyte population which is comprised of a large proportion of CD4$^-$CD8αβ$^-$CD8αα$^+$ T cells. Due to the heterogeneity, it has been challenging to identify or study a particular antigen-specific T cell clone from the population. Here we found that QFL T cells, a Vα3.2-expressing CD8$^+$ T cell population which specifically recognizes the Qa-1^b-FL9 ligand presented on ERAAP-KO cells, naturally resided in both the spleen and small intestine epithelium of naïve WT mice. Further characterization of QFL T cells revealed their unconventional phenotype, functionality and intimate association with gut microbiota.

Unlike conventional memory T cells which are generated upon encounter with their cognate peptide antigens on classical MHC molecules, 'innate' memory T cells arise under homeostatic conditions in response to neonatal lymphopenia, high levels of IL-4 or exposure to self-antigens in naïve mice (***Jameson et al., 2015***; ***Sprent et al., 2011***). Here, we found that splenic Vα3.2$^+$QFL T cells display a memory phenotype and the corresponding rapid effector function, but acquire this phenotype in a Qa-1^b dependent manner. Given the unique dependence on Qa-1^b expression for the phenotype imprinting of QFL T cells, it is possible that QFL T cells are exposed to transiently induced QFL epitope on cells due to various intracellular stressors that might affect ERAAP function. Alternatively, QFL T cells might cross-react with Qa-1^b presented FL9 homologue peptide(s). Indeed, we found that Vα3.2$^+$QFL T cells cross-reacted with one such variant of FL9 peptide (FL10) expressed in a commensal bacterium and presented by Qa-1^b. However, the Qa-1^b-FL10 ligand itself is unlikely to be directly associated with the memory imprinting for QFL T cells as these cells showed unaltered phenotype in germ-free mice. There might be other unidentified self-peptide(s) presented by Qa-1^b that are involved in the process. It is also possible that there is some level of degeneracy in the TCR-Qa-1^b interaction, so the precise peptide being presented is less critical than the presence of any peptide-Qa-1^b complex.

In line with a previous study, we observed that the Vα3.2-expressing CD8αβ$^+$ T population was comprised of a relatively larger proportion of memory phenotype cells in the spleen than the non-Vα3.2 expressing population (***Prasad et al., 2021***). In addition, these memory phenotype non-QFL Vα3.2$^+$CD8αβ$^+$ T cells were lost in Qa-1^b-KO mice. These results indicate that Vα3.2$^+$QFL T cells are likely only one prototypical example of Qa-1^b restricted Vα3.2$^+$CD8$^+$ T cells clones with memory phenotype and innate-like function. Strikingly, we detected abundant Vα3.2$^+$QFL T cells in small intestine epithelium which showed the signature phenotype of natIELs including expression of CD8αα and lack of CD4, CD8αβ, CD5 and CD90. Similar to the splenic population, while TAP is required for the presence of the population, the unconventional phenotype of Vα3.2$^+$QFL T cells in the gut is strongly Qa-1^b-dependent. It is so far reported that CD8αα$^+$ IELs can be restricted to K^{b}D^b, CD1d or even unknown MHC Ib molecules(***Mayans et al., 2014***; ***Ruscher et al., 2017***). Here by characterization of the gut Vα3.2$^+$QFL T cells, we showed evidence of abundant Qa-1^b-restricted TCRαβ$^+$ natIELs being present in the gut.

Functionally, the gut Vα3.2$^+$QFL T cells showed features consistent with their CD8αα$^+$ natIEL phenotype. Notably, although the siIEL Vα3.2$^+$QFL T cells showed delayed and reduced IFN-ɣ production in response to the cognate peptide, they displayed higher basal levels of intracellular IFN-ɣ than CD8αβ$^+$ IELs. It has been proposed that spontaneous IFN-ɣ secretion by IELs may be an important component of immunosurveillance at the mucosal surface, capable of identifying and eliminating transformed cells(***Carol et al., 1998***; ***Roberts et al., 1993***). Thus, siIEL QFL T cells may likewise be poised for immediate elimination of abnormal cells.

CD8αα$^+$ IELs are intrinsically programmed for innate functionality, as was shown by PMA/ionomycin induced production of high level of IFN-ɣ, CXCL2 etc.(***Van Kaer et al., 2014***). However, our observation of the relative hyporesponsiveness of siIEL Vα3.2$^+$QFL T to stimuli indicated that under physiological conditions, the activation of IELs was more complex and highly regulated as TCRs and inhibitory coreceptors such as CD8αα were engaged(***Cheroutre et al., 2008***; ***Madakamutil et al., 2004***). It is not surprising that the gut QFL T cells were functionally quiescent as these cells are constantly challenged by the microbial or dietary antigens from gut lumen(***Denning et al., 2007***). Cross-reaction between QFL T cells and peptide expressed in the commensal bacterium *P. pentosaceus* further supports this notion. Strikingly, monocolonization of the GF mice with *P. pentosaceus* was sufficient to restore gut Vα3.2$^+$QFL T cells that were lost in old GF mice. Of note, the control bacterium *L. johnsonni,* which lack FL10 expression, did not restore gut Vα3.2$^+$QFL T cells. Despite the evidence we remain cautious of other possible signals generated from colonization of the commensal bacterium, such as secretion of bacteriocins.

In conclusion, Vα3.2-expressing QFL T cells represent an unconventional population of Qa-1^b-restricted CD8$^+$ T cells which naturally reside at high frequency in small intestine epithelium. These cells have memory phenotype in the spleen and reveal the characteristics of natIELs in the gut. In addition, the fact that Vα3.2$^+$QFL T cross-reacts with FL9 homologue peptide expressed in a commensal bacterium suggests that these cells might be functionally versatile. Further study of the biological significance of these cells could potentially reveal the delicate equilibrium between gut microenvironment and immune system.

Acknowledgements

We thank P. Rhee at Shastri Lab, H. Ding at the JHU germ-free core facility for technical support. We thank Dr. L. Coscoy at University of California, Berkeley for providing cellular biology expertise, Dr. X. Li at Ragon Institute of MGH, MIT and Harvard for providing insights on prediction of peptide binding to unconventional MHC I molecules. This work was supported by grants from the National Institutes of Health (R01AI130210, R37AI060040, R01AI149341).

Methods

Mice

SPF wild-type C57BL/6J, H-2T23-deficient Qa-1^{b}-KO, C57BL/6-Tg (TcraTcrb)1100Mjb/J OT-1, or C57BL/6-Tg (UBC-GFP)30Scha/J B6.GFP mice were obtained from the Jackson Laboratory. QFL T TCR transgenic mice QFLTg were generated in the laboratory of E. Robey (University of California Berkeley, Berkeley, CA) and housed in our facility. GFP^{+}QFLTg mice were generated in our facility by crossing B6.GFP mice with QFLTg mice. SPF QFLTg_WT, SPF OT-1_WT and GF QFLTg_WT partial hematopoietic chimera mice were generated as previously described(***Ladi et al., 2008***). GF wild-type C57BL/6J and GF QFLTg_WT chimera mice were generated and maintained in the Johns Hopkins Germ-free Mouse Core Facility. Mice were housed and all procedures were done in accordance with protocols approved by Animal Care and Use Committee of the Johns Hopkins University School of Medicine.

Generation of the QFLTg mouse

The QFLTg TCR α-and β-chain sequences were cloned and amplified from the genomic DNA of BEko8Z hybridoma(***Guan et al., 2017***; ***Nagarajan et al., 2012***). The TCR α-chain was amplified with the forward primer 5'-AAAACCCGGGCCAAGGCTCAGCCATGCTCCTGG-3' and the reverse primer 5'-AAAAGCGGCCGCATACAACATTGGACAAGGATCCAAGCTAAAGAGAACTC-3'. The TCR β-chain was cloned with the forward primer 5'-AAAACTCGAGCCCGTCTGGAGCCTGATTCCA-3' and the reverse primer 5'-AAAACCGCGGGGGACCCAGGAATTTGGGTGGA-3'. The TCR α-chain DNA fragment was cloned into pTα cassette vector by inserting it between the XmaI and NotI sites, while the TCR β-chain DNA fragment was cloned into pTβ cassette vector in between the XhoI and SacII sites(***Kouskoff et al., 1995***). The ampicillin resistance gene was removed from pTα and pTβ cassette by EarI enzyme digest. The QFLTg mice were generated on C57BL/6J background in the Cancer Research Laboratory Gene Targeting Facility at UC Berkeley under standard procedures. Founder mice were identified by flow cytometry and PCR genotyping of tail genomic DNA using primers mentioned above.

Antibodies, cell lines and peptides

Antibody for flow cytometry were from BioLegend (anti-CD45(30-F11), anti-CD19(1D3/CD19), anti-TCRβ(H57-597), anti-CD8β(53-5.8), anti-Vα3.2(RR3-16), anti-Vα2(B20.1), anti-CD90.2(53-2.1), anti-CD5(53-7.3), anti-IFN-ɣ(XMG1.2), anti-CD62L(MEL-14) and BD Biosciences (anti-CD4(RM4-5), anti-CD8α (53-6.7), anti-CD44(IM7)). BEko8Z, L-Qa-1^{b} or Lmtk^{-} cells were maintained as previously described(***Nagarajan et al., 2012***). Peptides were obtained from GenScript. The purity of SL8, FL9 and FL10 peptides were ⩾98%.

Generation of the QFL-dextramer

Qa-1^{b}-FL9 (QFL) monomers were synthesized by the Tetramer Core Facility of the US National Institutes of Health. Phycoerythrin (PE)- or allophycocyanin (APC)-conjugated streptavidin were obtained from Agilent. The QFL dextramers were generated following the 'dextran doping' technique(***Bethune et al., 2017***). The QFL monomers were incubated with PE or APC conjugated streptavidin at a molar ratio of 3:1 at 4°C for 10min followed by addition of biotinylated dextran molecular weight 500kDa at a molar ratio of 1:20 with respect to streptavidin. The mixture was further incubated at 4°C for ≧1h before being used in experiments.

Isolation of IELs

Small intestinal IELs were isolated following an established protocol with minor modifications (***Qiu et al., 2018***). In brief, the small intestine with Payer's patches removed were cut into appropriate length. The fecal content and mucus were removed by expelling with the flat side of forceps followed by flushing with PBS. The intestine was cut open longitudinally to reveal the

epithelium and further cut laterally into ~2cm pieces. The intestine pieces were then placed in 25ml warmed dithioerythritol (DTE) solution (Ca^{2+}- and Mg^{2+}-free Hanks balanced salt solution, HEPES-bicarbonate buffer, 10% FCS) in 50ml conical tube and were shaken at 75rpm 37°C for 20min. The tube was vortexed for 10s before the supernatant was transferred into a new 50ml conical tube through a 70μM cell strainer. The cells were palleted and resuspend in 44% Percoll solution (44% Percoll in RPMI 1640). Density gradient was generated by underlaying the cell suspension with 67% Percoll solution (67% Percoll in RPMI 1640). The gradient cell suspension was further centrifuged at 1600 × g for 20 min at RT without using the brake. The layer of cells at the 44% and 67% interphase were thus collected as IELs.

Enrichment for dextramer-positive cells

Splenic dextramer-positive cells were enriched as previously described(***Nagarajan et al., 2012***). IELs were resuspend in 100μl sorter buffer (0.1% sodium azide and 5% FCS in PBS). PE or APC labeled QFL dextramers were added at a final dilution of 1:100. Cells were incubated at room temperature for 45 min, then were washed twice with 3ml of sorter buffer. 20μl of anti-PE and 20μl of anti-APC microbeads (Miltenyi Biotec) were added into cells resuspended in 450μl of sorters buffer, followed by incubation of 20 min at 4°C. Cells were washed twice with 3ml sorter buffer. The PE- and APC-labeled cells were positively selected by passing through LS magnetic columns (Miltenyi Biotec). The entire isolated population was stained with anti-CD45, anti-CD19, anti-TCRβ, anti-CD4, anti-CD8α and anti-CD8β. QFL T cells were gated as $CD45^{+}CD19^{-}TCR\beta^{+}CD4^{-}$ QFL-Dex-PE^{+}QFL-Dex-APC^{+} population. The absolute numbers and frequencies of the cells were calculated based on a fixed number of CountBright Beads (Thermo Fisher) added into each sample.

Cytokine stimulation and proliferation assay

Splenocytes or small intestinal IELs isolated from QFLTg or OT-1 mice were depleted of non-T cells using Pan T isolation Kit II (Miltenyi Biotec). The negatively selected T cells were then labeled with 5μM Cell Tracing Violet (CTV) (Thermo Fisher) and adjusted to the concentration of 10^6/ml. 10^6 of the CTV labeled T cells were stimulated *in vitro* for 3 or 5 days in cultures containing 100ng/ml IL15 (BioLegend) or a combination of 100ng/ml IL7 (BioLegend) and 100ng/ml IL18 (BioLegend) in 24-well plate at 37°C. Proliferation of cells were measured by dilution of CTV on flow cytometer.

CTL assay

Lymphocytes isolated from the spleen or siIEL compartment of naïve QFLTg_WT or OT-1_WT chimera mice were cultured *in vitro* with 2μM of FL9 or SL8 peptide respectively together with GolgiPlug (BD Biosciences) for 4.5h. WT splenocytes were supplemented into siIEL cultures as APCs. Cells were then washed and stained for surface markers. For measurement of IFN-ɣ production, cells were fixed and permeabilized using Fixation/Permeabilization Kit (BD Biosciences) and stained for intracellular IFN-ɣ.

Hybridoma assay

10^5 of BEko8Z hybridoma cells were cocultured with 10^5 of L-Qa-1^b or Lmtk-cells in medium containing peptides of indicated concentrations in 96-well plates at 37°C for 12 hours. T cell response was determined by cleavage of the chromogenic LacZ substrate chlorophenol red-β-D-galactopyranoside (CPRG, Millipore Sigma) by TCR-induced LacZ and measure by spectrophotometry as presented by absorbance at 595 nm (A595) (***Sanderson et al., 1994***). Background signals were subtracted by measurement of absorbance at 655nm.

Commensal culture and colonization

Pediococcus pentosaceus Mees (33314) and *Lactobacillus johnsonii* (33200) were obtained from ATCC. The bacteria were grown overnight at 37°C in 416 Lactobacilli MRS Broth (BD Biosciences). GF QFLTg_WT chimera mice were gavaged with 200µl of 2×10^8/ml CFU of *P. pentosaceus Mees* at 8 weeks of age. GF WT mice were gavaged with 200µl of 2×10^8/ml CFU of *P. pentosaceus Mees* or *L. johnsonii* at 8 and 10 weeks of age. Fecal pallets collected from the colonized mice were homogenized in 416 Lactobacilli MRS Broth, and the associated mice were determined by plating the appropriate dilution of homogenate on 416 Lactobacilli MRS agar plates. Bacterial colonization efficiency was determined by whole shotgun metagenomic sequencing of fecal pallets collected from the colonized mice at 16 weeks of age (TransnetYX Microbiome).

References

Belkaid Y., Hand T.W (2014) **Role of the microbiota in immunity and inflammation** *Cell* **157**:121–141 https://doi.org/10.1016/j.cell.2014.03.011

Bethune M.T., Comin-Anduix B., Fu Y.-H.H., Ribas A., Baltimore D (2017) **Preparation of peptide–MHC and T-cell receptor dextramers by biotinylated dextran doping** *Biotechniques* **62**:123–130 https://doi.org/10.2144/000114525

Blanchard N., Shastri N (2008) **Coping with loss of perfection in the MHC class I peptide repertoire** *Curr Opin Immunol* **20**:82–88 https://doi.org/10.1016/j.coi.2007.12.004

Blum J.S., Wearsch P.A., Cresswell P (2013) **Pathways of antigen processing** *Annu Rev Immunol* **31**:443–473 https://doi.org/10.1146/annurev-immunol-032712-095910

Carol M., Lambrechts A., Van Gossum A., Libin M., Goldman M., Mascart-Lemone F. (1998) **Spontaneous secretion of interferon gamma and interleukin 4 by human intraepithelial and lamina propria gut lymphocytes** *Gut* **42**:643–649 https://doi.org/10.1136/gut.42.5.643

Cheroutre H., Lambolez F (2008) **Doubting the TCR coreceptor function of CD8αα** *Immunity* **28**:149–159 https://doi.org/10.1016/j.immuni.2008.01.005

Cheroutre H., Lambolez F., Mucida D (2011) **The light and dark sides of intestinal intraepithelial lymphocytes** *Nat Rev Immunol* **11**:445–456 https://doi.org/10.1038/nri3007

Das G., Gould D.S., Augustine M.M., Fragoso G., Sciutto E., Stroynowski I., Van Kaer L., Schust D.J., Ploegh H., Janeway C.A. (2000) **Qa-2-dependent selection of CD8αα T cell receptor αβ+ cells in murine intestinal intraepithelial lymphocytes** *J Exp Med* **192**:1521–1528 https://doi.org/10.1084/jem.192.10.1521

Das G., Janeway C.A. (1999) **Development of CD8αα and CD8αβ T cells in major histocompatibility complex class I-deficient mice** *J Exp Med* **190**:881–884 https://doi.org/10.1084/jem.190.6.881

Das G., Janeway C.A. (2003) **MHC specificity of iIELs** *Trends Immunol* **24**:88–93 https://doi.org/10.1016/s1471-4906(02)00036-4

Denning T.L., Granger S.W., Mucida D., Graddy R., Leclercq G., Zhang W., Honey K., Rasmussen J.P., Cheroutre H., Rudensky A.Y., et al. (2007) **Mouse TCRαβ+CD8αα intraepithelial lymphocytes express genes that down-regulate their antigen reactivity and suppress immune responses** *J Immunol* **178**:4230–4239 https://doi.org/10.4049/jimmunol.178.7.4230

Donaldson G.P., Lee S.M., Mazmanian S.K (2016) **Gut biogeography of the bacterial microbiota** *Nat Rev Microbiol* **14**:20–32 https://doi.org/10.1038/nrmicro3552

Faria A.M.C., Reis B.S., Mucida D (2017) **Tissue adaptation: Implications for gut immunity and tolerance** *J Exp Med* **214**:1211–1226 https://doi.org/10.1084/jem.20162014

Godfrey D.I., Uldrich A.P., McCluskey J., Rossjohn J., Moody D.B (2015) **The burgeoning family of unconventional T cells** *Nat Immunol* **16**:1114–1123 https://doi.org/10.1038/ni.3298

Grandea A.G, Golovina T.N., Hamilton S.E., Sriram V., Spies T., Brutkiewicz R.R., Harty J.T., Eisenlohr L.C., Van Kaer L. (2000) **Impaired assembly yet normal trafficking of MHC class I molecules in Tapasin mutant mice** *Immunity* **13**:213–222 https://doi.org/10.1016/s1074-7613(00)00021-2

Guan J., Peske J.D., Taylor J.A., Shastri N (2021) **The nonclassical immune surveillance for ERAAP function** *Curr Opin Immunol* **70**:105–111 https://doi.org/10.1016/j.coi.2021.05.008

Guan J., Yang S.J., Gonzalez F., Yin Y., Shastri N (2017) **Antigen Processing in the Endoplasmic Reticulum Is Monitored by Semi-Invariant αβ TCRs Specific for a Conserved Peptide-Qa-1b MHC Class Ib Ligand** *J Immunol* **198**:2017–2027 https://doi.org/10.4049/jimmunol.1600764

Hammer G.E., Gonzalez F., Champsaur M., Cado D., Shastri N (2006) **The aminopeptidase ERAAP shapes the peptide repertoire displayed by major histocompatibility complex class I molecules** *Nat Immunol* **7**:103–112 https://doi.org/10.1038/ni1286

Hammer G.E., Gonzalez F., James E., Nolla H., Shastri N (2007) **In the absence of aminopeptidase ERAAP, MHC class I molecules present many unstable and highly immunogenic peptides** *Nat Immunol* **8**:101–108 https://doi.org/10.1038/ni1409

Hammer G.E., Kanaseki T., Shastri N (2007) **The final touches make perfect the peptide-MHC class I repertoire** *Immunity* **26**:397–406 https://doi.org/10.1016/j.immuni.2007.04.003

Jameson S.C., Lee Y.J., Hogquist K.A (2015) **Innate memory T cells** *Adv Immunol* **126**:173–213 https://doi.org/10.1016/bs.ai.2014.12.001

Klose C.S., Blatz K., d'Hargues Y., Hernandez P.P., Kofoed-Nielsen M., Ripka J.F., Ebert K., Arnold S.J., Diefenbach A., Palmer E., et al. (2014) **The transcription factor T-bet is induced by IL-15 and thymic agonist selection and controls CD8αα+ intraepithelial lymphocyte development** *Immunity* **41**:230–243 https://doi.org/10.1016/j.immuni.2014.06.018

Kouskoff V., Signorelli K., Benoist C., Mathis D (1995) **Cassette vectors directing expression of T cell receptor genes in transgenic mice** *J Immunol Methods* **180**:273–280 https://doi.org/10.1016/0022-1759(95)00002-r

Ladi E., Herzmark P., Robey E (2008) **In situ imaging of the mouse thymus using 2-photon microscopy** *J Vis Exp* https://doi.org/10.3791/652

Macpherson A.J., Harris N.L (2004) **Interactions between commensal intestinal bacteria and the immune system** *Nature Reviews Immunology* **4**:478–485 https://doi.org/10.1038/nri1373

Madakamutil L.T., Christen U., Lena C.J., Wang-Zhu Y., Attinger A., Sundarrajan M., Ellmeier W., von Herrath M.G., Jensen P., Littman D.R., et al. (2004) **CD8αα-mediated survival and differentiation of CD8 memory T cell precursors** *Science* **304**:590–593 https://doi.org/10.1126/science.1092316

Mayans S., Stepniak D., Palida Sakina F., Larange A., Dreux J., Arlian Britni M., Shinnakasu R., Kronenberg M., Cheroutre H., Lambolez F (2014) **αβT Cell Receptors Expressed by CD4–CD8αβ– Intraepithelial T Cells Drive Their Fate into a Unique Lineage with Unusual MHC Reactivities** *Immunity* **41**:207–218 https://doi.org/10.1016/j.immuni.2014.07.010

Mota-Santos T., Masmoudi H., Voegtle D., Freitas A., Coutinho A., Cazenave P.A (1990) **Divergency in the specificity of the induction and maintenance of neonatal suppression** *Eur J Immunol* **20**:1717–1721 https://doi.org/10.1002/eji.1830200814

Nagarajan N.A., de Verteuil D.A., Sriranganadane D., Yahyaoui W., Thibault P., Perreault C., Shastri N. (2016) **ERAAP Shapes the Peptidome Associated with Classical and Nonclassical MHC Class I Molecules** *J Immunol* **197**:1035–1043 https://doi.org/10.4049/jimmunol.1500654

Nagarajan N.A., Gonzalez F., Shastri N (2012) **Nonclassical MHC class Ib-restricted cytotoxic T cells monitor antigen processing in the endoplasmic reticulum** *Nat Immunol* **13**:579–586 https://doi.org/10.1038/ni.2282

Okazawa A., Kanai T., Nakamaru K., Sato T., Inoue N., Ogata H., Iwao Y., Ikeda M., Kawamura T., Makita S., et al. (2004) **Human intestinal epithelial cell-derived interleukin (IL)-18, along with IL-2, IL-7 and IL-15, is a potent synergistic factor for the proliferation of intraepithelial lymphocytes** *Clin Exp Immunol* **136**:269–276 https://doi.org/10.1111/j.1365-2249.2004.02431.x

Park S.H., Guy-Grand D., Lemonnier F.A., Wang C.R., Bendelac A., Jabri B (1999) **Selection and expansion of CD8αα+ T cell receptor αβ+ intestinal intraepithelial lymphocytes in the absence of both classical major histocompatibility complex class I and nonclassical CD1 molecules** *J Exp Med* **190**:885–890 https://doi.org/10.1084/jem.190.6.885

Prasad M., Wojciech L., Brzostek J., Hu J., Chua Y.L., Tung D.W.H., Yap J., Rybakin V., Gascoigne N.R.J (2021) **Expansion of an Unusual Virtual Memory CD8+ Subpopulation Bearing Valpha3.2 TCR in Themis-Deficient Mice** *Front Immunol* **12** https://doi.org/10.3389/fimmu.2021.644483

Qiu Z., Sheridan B.S (2018) **Isolating Lymphocytes from the Mouse Small Intestinal Immune System** *J Vis Exp* **10**

Roberts A.I., O'Connell S.M., Biancone L., Brolin R.E., Ebert E.C (1993) **Spontaneous cytotoxicity of intestinal intraepithelial lymphocytes: clues to the mechanism** *Clin Exp Immunol* **94**:527–532 https://doi.org/10.1111/j.1365-2249.1993.tb08229.x

Round J.L., Mazmanian S.K (2009) **The gut microbiota shapes intestinal immune responses during health and disease** *Nat Rev Immunol* **9**:313–323 https://doi.org/10.1038/nri2515

Ruscher R., Kummer R.L., Lee Y.J., Jameson S.C., Hogquist K.A (2017) **CD8αα intraepithelial lymphocytes arise from two main thymic precursors** *Nat Immunol* **18**:771–779 https://doi.org/10.1038/ni.3751

Salio M., Silk J.D., Jones E.Y., Cerundolo V (2014) **Biology of CD1- and MR1-restricted T cells** *Annu Rev Immunol* **32**:323–366 https://doi.org/10.1146/annurev-immunol-032713-120243

Sanderson S., Shastri N (1994) **LacZ inducible, antigen/MHC-specific T cell hybrids** *Int Immunol* **6**:369–376 https://doi.org/10.1093/intimm/6.3.369

Schluns K.S., Lefrancois L (2003) **Cytokine control of memory T-cell development and survival** *Nat Rev Immunol* **3**:269–279 https://doi.org/10.1038/nri1052

Serwold T., Gonzalez F., Kim J., Jacob R., Shastri N (2002) **ERAAP customizes peptides for MHC class I molecules in the endoplasmic reticulum** *Nature* **419**:480–483 https://doi.org/10.1038/nature01074

Shastri N., Cardinaud S., Schwab S.R., Serwold T., Kunisawa J (2005) **All the peptides that fit: the beginning, the middle, and the end of the MHC class I antigen-processing pathway** *Immunol Rev* **207**:31–41 https://doi.org/10.1111/j.0105-2896.2005.00321.x

Shastri N., Schwab S., Serwold T (2002) **Producing nature's gene-chips: the generation of peptides for display by MHC class I molecules** *Annu Rev Immunol* **20**:463–493 https://doi.org/10.1146/annurev.immunol.20.100301.064819

Sprent J., Surh C.D (2011) **Normal T cell homeostasis: the conversion of naive cells into memory-phenotype cells** *Nat Immunol* **12**:478–484 https://doi.org/10.1038/ni.2018

Van Kaer L., Algood H.M.S., Singh K., Parekh V.V., Greer M.J., Piazuelo M.B., Weitkamp J.H., Matta P., Chaturvedi R., Wilson K.T., et al. (2014) **CD8αα⁺ innate-type lymphocytes in the intestinal epithelium mediate mucosal immunity** *Immunity* **41**:451–464 https://doi.org/10.1016/j.immuni.2014.08.010

Van Kaer L., Ashton-Rickardt P.G., Eichelberger M., Gaczynska M., Nagashima K., Rock K.L., Goldberg A.L., Doherty P.C., Tonegawa S. (1994) **Altered peptidase and viral-specific T cell response in LMP2 mutant mice** *Immunity* **1**:533–541 https://doi.org/10.1016/1074-7613(94)90043-4

Van Kaer L., Ashton-Rickardt P.G., Ploegh H.L., Tonegawa S. (1992) **TAP1 mutant mice are deficient in antigen presentation, surface class I molecules, and CD4-8+ T cells** *Cell* **71**:1205–1214 https://doi.org/10.1016/s0092-8674(05)80068-6

Author information

Jian Guan
Department of Pathology and the Institute of Cell Engineering, Johns Hopkins University School of Medicine, Baltimore, MD 21287, USA
For correspondence: jian.guan.cc@outlook.com
ORCID iD: 0000-0002-0118-6578

J. David Peske
Department of Pathology and the Institute of Cell Engineering, Johns Hopkins University School of Medicine, Baltimore, MD 21287, USA

Michael Manoharan Valerio
Division of Immunology and Molecular Medicine, Department of Molecular and Cell Biology, University of California, Berkeley, Berkeley, CA 94720, USA

Chansu Park
Department of Pathology and the Institute of Cell Engineering, Johns Hopkins University School of Medicine, Baltimore, MD 21287, USA

Ellen A. Robey
Division of Immunology and Molecular Medicine, Department of Molecular and Cell Biology, University of California, Berkeley, Berkeley, CA 94720, USA

Scheherazade Sadegh-Nasseri
Department of Pathology and the Institute of Cell Engineering, Johns Hopkins University School of Medicine, Baltimore, MD 21287, USA
For correspondence: ssadegh@jhmi.edu

Nilabh Shastri
Department of Pathology and the Institute of Cell Engineering, Johns Hopkins University School of Medicine, Baltimore, MD 21287, USA

Editors

Reviewer #1 (Public Review):

Guan et al. explored the mechanisms responsible for the development, maintenance, and functional properties of a specific subset of unconventional T cells expressing a Va3.2 T cell receptor that recognizes a peptide, QFL, presented by the class Ib protein Qa-1. Prior studies from this group showed that cells from mice deficient in the ER protease ERAAP elicit responses in wild-type animals enriched for Qa-1-restricted CD8 T cells. They further showed that a significant proportion of these responses were directed against the QFL peptide derived from a conserved protein with incompletely understood functions. Many of these so-called QFL T cells expressed Va3.2-Ja21, were present in the spleen of wild-type mice, and exhibited a memory-like phenotype. Due to their relatively low frequency and weak staining with Qa-1 tetramers, analyzing QFL T cells has been challenging. Therefore, the authors generated dextramers, which permitted them to more rigorously identify these cells. They confirmed some of their previous findings and further showed that Va3.2+ and Va3.2- QFL T cells were present in the intestinal epithelium, where they also express CD8alpha homodimers, a characteristic of most small intestinal intraepithelial lymphocytes (siIELs), and most similar to the so-called natural siIELs that acquire their innate functions in the thymus. The authors show that TAP but not Qa-1 or ERAAP expression are required for the development of these cells, and both Qa-1 and ERAAP are required for the natural siIEL phenotype. Some of these findings were confirmed using a new TCR transgenic mouse expressing the QFL TCR. They further show that retention but not homing of QFL T cells to the intestinal epithelium involves commensal microorganisms, and using in silico approaches, they identify a commensal that contains a peptide similar to QFL that can activate QFL T cells. Finally, they show that this organism, P. pentosaceus, can promote gut retention of QFL T cells when it is introduced into germ-free mice. From these findings, the authors conclude that the microbiota influences the maintenance of Qa-1-restricted T cells.

Comments:
1. Overall, the authors employ a number of new reagents and elegant approaches to explore the development, maintenance, and functional properties of QFL T cells.
2. Generally, conclusions made are well supported by the data presented.
3. One limitation of the work is that the immunological functions of QFL T cells remain unclear.
4. The work covers a lot of ground (intestinal IELs, unconventional T cells, innate/virtual memory T cells, Qa-1/HLA-E, etc) that may not be familiar to many readers.
5. A few questions remain:
a) Regarding the results for TAP knockout animals, since Qa-1 does not appear to be required for QFL T cell development, the absence of these cells in TAP KO mice cannot be easily

explained.
b) The Va3.2 T cells display similarities with previously identified innate/virtual memory T cells, some of which require IL-4 production by CD1d-restricted NKT cells for their intrathymic development, which is not fully discussed.
c) Qa-1/peptide complexes may also be recognized by CD94/NKG2 (both inhibitory and activating) receptors on NK cells and subsets of CD8 T cells, which may complicate data interpretation, but is not noted in the text.
d) Are these conclusions relevant to the human homolog of Qa-1, HLA-E?

Reviewer #2 (Public Review):

Summary:
CD8+ QFL T cells recognize a peptide, FYAEATPML (FL9), presented on Erap1-deficient cells. QFL T cells are present at a high frequency in the spleen of naïve mice. They express an antigen-experienced phenotype, and about 80% express an invariant TCRα chain Vα3.2Jα21.

Here, Guan and colleagues report that QFL T cells are present not only in the spleen but also in the intestinal epithelium, where they display several phenotypic and functional peculiarities. The establishment of spleen and gut Vα3.2+ QFL T cells is TAP-dependent, and their phenotype is regulated by the presence/absence of Qa-1b and Erap1. Maintenance of gut Vα3.2+ QFL T cells depends on the gut microbiota and is associated with colonization by Pediococcus pentosaceus.

Strengths:
This article contains in-depth studies of a peculiar and interesting subset of unconventional CD8 T cells, based partly on generating two novel TCR-transgenic models.

The authors discovered a clear relation between the gut microbiome and the maintenance of gut QFL T cells. One notable observation is that monocolonization of the gut with Pediococcus pentosaceus is sufficient to sustain gut QFL T cells.

Weaknesses:
In the absence of immunopeptidomic analyses, the presence or absence of the FL9 peptide on various cell types is inferred based on indirect evidence.

Analyses of the homology between the FL9 and bacterial peptides were limited to two amino acid residues (P4 and P6).

The potential function of QFL T cells remains elusive.

Reviewer #3 (Public Review):

The authors investigate the role of commensal microbes and molecules in the antigen presentation pathway in the development and phenotype of CD8 T cells specific for the Qa-1b-restricted peptide FL9 (QFL). The studies track both endogenous QFL-specific T cells and utilize a recently generated TCR transgenic model. The authors confirm that QFL-specific T cells in the spleen and small intestine intraepithelial lymphocyte (IEL) pool show an antigen-experienced phenotype as well as unique phenotypic and innate-like functional traits, especially among CD8+ T cells expressing Va3.2+ TCRs. They find that deficiency in the TAP transporter leads to almost complete loss of QFL-specific T cells but that loss of either Qa1 or the ERAAP aminopeptidase does not impact QFL+ T cell numbers but does cause them to maintain a more conventional, naïve-like phenotype. In germ-free (GF) mice, the QFL-specific T cells are present at similar numbers and with a similar phenotype to SPF animals, but in older animals (>18w) there is a notable loss of IEL QFL-specific cells. This drop can be avoided by neonatal colonization of GF mice with the commensal microbe Pediococcus pentosaceus but not a different commensal, Lactobacillus johnsonii, and the authors show that P.

pentosaceus encodes a peptide that weakly stimulates QFL-specific T cells, while the homologous peptide from L. johnsonii does not stimulate such cells.

This study provides new insights into the way in which the differentiation, phenotype, and function of CD8+ T cells specific for Qa-1b/FL9 is regulated by peptide processing and Qa1 expression, and by interactions with the microbiota. The approaches are well designed, the data compelling, and the interpretation, for the most part, appropriate. There are a few relatively minor concerns.

1. For most of the report, the authors use a set of phenotypic traits to highlight the unique features of QFL-specific CD8+ T cells - specifically, CD44high, CD8aa+ve, CD8ab-ve. In Supp. Fig. 4, however, completely distinct phenotypic characteristics are presented, indicating that IEL QFL-specific T cells are CD5low, Thy-1low. No explanation is provided in the text about whether this is a previously reported phenotype, whether any elements of this phenotype are shared with splenic QFL T cells, what significance the authors ascribe to this phenotype (and to the fact that Qa1-deficiency leads to a more conventional Thy-1+ve, CD5+ve phenotype), and whether this altered phenotype is also seen in ERAAP-deficient mice. At least some explanation for this abrupt shift in focus and integration with prior published work is needed. On a related note, CD5 expression is measured in splenic QFL-specific CD8+ T cells from GF vs SPF mice (Supp. Fig. 9), to indicate that there is no phenotypic impact in the GF mice - but from Supp. Fig. 4, it would seem more appropriate to report CD5 expression in QFL-specific cells from the IEL, not the spleen.

2. The authors suggest the finding that QFL-specific cells from ERAAP-deficient mice have a more "conventional" phenotype indicates some form of negative selection of high-affinity clones (this result being somewhat unexpected since ERAAP loss was previously shown to increase the presentation of Qa-1b loaded with FL9, confirmed in this report). It is not clear how this argument aligns with the data presented, however, since the authors convincingly show no significant reduction in the number of QFL-specific cells in ERAAP-knockout mice (Fig. 3a), and their own data (e.g. Fig. 2a) do not suggest that CD44 expression correlates with QFL-multimer staining (as a surrogate for TCR affinity/avidity). Is there some experimental basis for suggesting that ERAAP-deficient lacks a subset of high-affinity QFL-specific cells?

3. The rationale for designing FL9 mutants, and for using these data to screen the proteomes of various commensal bacteria needs further explanation. The authors propose P4 and P6 of FL9 are likely to be "critical" but do not explain whether they predict these to be TCR or Qa-1b contact sites. Published data (e.g., PMID: 10974028) suggest that multiple residues contribute to Qa-1b binding, so while the authors find that P4A completely lost the ability to stimulate a QFL-specific hybridoma, it is unclear whether this is due to the loss of a TCR- or a Qa-1-contact site (or, possibly, both). This could easily be tested - e.g., by determining whether P4A can act as a competitive inhibitor for FL9-induced stimulation of BEko8Z (and, ideally, other Qa-1b-restricted cells, specific for distinct peptides). Without such information, it is unclear exactly what is being selected in the authors' screening strategy of commensal bacterial proteomes. This, of course, does not lessen the importance of finding the peptide from P. pentosaceus that can (albeit weakly) stimulate QFL-specific cells, and the finding that association with this microbe can sustain IEL QFL cells.